



Geochemical Characteristics and Paleoenvironmental Significance of the Ordovician Paleokarst Reservoir in the Maigaiti Slope of Tarim Basin

Qingyu Zhang^{1,2,3}, Liang Bin^{2,3}, Qin Fengrui^{2,3*}, Cao Jianwen^{1,2,3}, Dan Yong^{2,3}, Hao Yanzhen^{2,3}, Li Jingrui^{2,3}, Muhammad Aqeel Ashraf⁴

¹School of Environmental Studies, China University of Geosciences, Wuhan 430074, China;

²Institute of Karst Geology, Chinese Academy of Geological Sciences/Karst Dynamics Laboratory, MLR & GZAR, Guilin 541004;

³International Research Center on Karst under the Auspices of UNESCO, Guilin, Guangxi 541004

⁴ Faculty of Science and Natural Resources, University Malaysia Sabah 88400 Kota Kinabalu, Sabah, Malaysia

* Corresponding author: Qin Fengrui, email: qinfengrui@karst.ac.cn

ABSTRACT

The Ordovician carbonatites of the Maigaiti slope have formed the conditions for the development of large oil and gas fields with karst reservoirs. This study systematically analyzed the isotopic characteristics of carbon, oxygen, and strontium and enrichment trace elements regularity to examine the geochemical features of the paleo-karstification products, various periods of paleo-karstification, and paleoenvironmental conditions of the Ordovician. Affected by terrigenous clasts, the Lianglitage Formation is composed of limestone with a relatively high $87\text{Sr}/86\text{Sr}$ value and a frequently fluctuating sea level, which exhibits an overall increasing-to-decreasing trend variation. Of all samples affected by the atmospheric freshwater leaching effect, $\delta^{18}\text{O}$ values were negative, and $\delta^{13}\text{C}$ values varied greatly toward both ends. The fissure/cave infills were rich in Fe and Mn but poor in Sr, and the Sr/Ba value was considerably less than 1, which confirms the existence of ancient weathered crust and the development of an atmospheric freshwater karst environment. Four different paleo-karstification periods were identified according to the carbon and oxygen isotopic characteristics of calcite. Combined with the trace element characteristics of the infills, the paleo-karstification in the Yingshan Formation was subdivided based on three hydrological environment conditions. Erosion modification of buried acid compaction-released water from late-period corrosion pores, caves, and fissures formed by syndiagenetic paleo-karstification and weathered crust bare paleo-karstification due to atmospheric freshwater leaching can significantly improve the reserving and permeability characteristics of the karst reservoir to develop a large paleokarst reservoir.

Keywords: Ordovician paleokarst, paleoenvironment, carbon–oxygen–strontium isotope, trace elements, Maigaiti slope, Tarim Basin

Record

Manuscript received: 12/11/2015

Accepted for publication: 05/02/2016

How to cite item

Qingyu, Z., Bin, L., Fengrui, Q., Jianwen, C., Yong, D., Yanzhen, H., Jingrui, L., & Ashraf, M.A. (2016). Geochemical Characteristics and Paleoenvironmental Significance of the Ordovician Paleokarst Reservoir in the Maigaiti Slope of Tarim Basin. *Earth Sciences Research Journal*, 20(1), L1-L10. doi: <http://dx.doi.org/10.15446/esrj.v20n1.54142>

1 Introduction

Paleo-karstification is a transformative process of soluble rocks by the action of ancient surface water and groundwater and the sum of resulting surface and underground geologic phenomena (Wang and Al-Aasm, 2002; Wen et al., 2014). In domestic and global carbonatite rock strata, reservoirs formed by the result of paleo-karstification are very common and often develop large to very large oil and gas fields (Yang et al., 2011) that contain rich oil and gas resources (Kerans, 1988; Guo, 1993; Loucks, 1999; Chen et al., 2004). Paleokarst carbonatite reservoirs are widely distributed in China. With the continuously expanding application of new technology and new methods for petroleum exploration, a large number of paleokarst reservoirs have been found in the Tarim (Zhang et al., 2004; Wu et al., 2012), Qaidam (Feng et al., 2013), Ordos (Xia et al., 2007), and Sichuan basins (Zhang et al., 2011). These findings have led to the development of various medium- and large-scale oil and gas fields such as the Tahe, Lunnan, Changqing, and Weiyuan. This outlook indicates that the paleokarst carbonatite reservoirs in China are highly promising with significant exploration potential (Jin et al., 2006). Therefore, expanded research into paleokarst reservoirs in marine oil and gas exploration is crucial (Jia and Cai, 2004; Liu, 2007; Su et al., 2010).

In recent years, researchers have applied geochemical characteristics in paleokarst reservoir research and have greatly promoted global research on paleokarst and diagenesis fluids (Shields et al., 2003; Veizer et al., 1999; Liu et al., 2012; Yan et al., 2005; Huang et al., 2008).

The Maigaiti slope is located in the northern slope zone of the southwestern depression of the Tarim Basin, where oil and gas exploration remains at a relatively low level. Only the Bashituopu oilfield was found in the western Maigaiti slope (Liu et al., 2004). Nevertheless, a series of Ordovician marine carbonatite oil and gas fields has been discovered in the northern and central paleohigh areas of the Tarim Basin (Kang, 2007; Zhou, 2010). Therefore, the discovery of replacement areas with a similar paleohigh background is of great importance in the exploration and development of oil and gas fields (Shi et al., 2014).

Previous research has indicated that the Maigaiti slope and its marginal area developed paleohighs and formed multiple sets of reservoir-cap combinations, leading to migration and accumulation of hydrocarbons during various periods (Li, 2009; Zhao, 2012; Tian, 2013). However, this exploration has not achieved a breakthrough in the past 20 years. Also, early research and exploration of the Maigaiti slope were focused on the Carboniferous system as a major target layer (Zheng, 1995; He et al, 1999; Zhou et al., 2006); Yang et al., 2007). No studies on the formation

1 Introduction

Paleo-karstification is a transformative process of soluble rocks by the action of ancient surface water and groundwater and the sum of resulting surface and underground geologic phenomena (Wang and Al-Aasm, 2002; Wen et al., 2014). In domestic and global carbonatite rock strata, reservoirs formed by the result of paleo-karstification are very common and often develop large to very large oil and gas fields (Yang et al., 2011) that contain rich oil and gas resources (Kerans, 1988; Guo, 1993; Loucks, 1999; Chen et al., 2004). Paleokarst carbonatite reservoirs are widely distributed in China. With the continuously expanding application of new technology and new methods for petroleum exploration, a large number of paleokarst reservoirs have been found in the Tarim (Zhang et al., 2004; Wu et al., 2012), Qaidam (Feng et al., 2013), Ordos (Xia et al., 2007), and Sichuan basins (Zhang et al., 2011). These findings have led to the development of various medium- and large-scale oil and gas fields such as the Tahe, Lunnan, Changqing, and Weiyuan. This outlook indicates that the paleokarst carbonatite reservoirs in China are highly promising with significant exploration potential (Jin et al., 2006). Therefore, expanded research into paleokarst reservoirs in marine oil and gas exploration is crucial (Jia and Cai, 2004; Liu, 2007; Su et al., 2010).

In recent years, researchers have applied geochemical characteristics in paleokarst reservoir research and have greatly promoted global research on paleokarst and diagenesis fluids (Shields et al., 2003; Veizer et al., 1999; Liu et al., 2012; Yan et al., 2005; Huang et al., 2008).

The Maigaiti slope is located in the northern slope zone of the southwestern depression of the Tarim Basin, where oil and gas exploration remains at a relatively low level. Only the Bashituopu oilfield was found in the western Maigaiti slope (Liu et al., 2004). Nevertheless, a series of Ordovician marine carbonatite oil and gas fields has been discovered in the northern and central paleohigh areas of the Tarim Basin (Kang, 2007; Zhou, 2010). Therefore, the discovery of replacement areas with a similar paleohigh background is of great importance in the exploration and development of oil and gas fields (Shi et al., 2014).

Previous research has indicated that the Maigaiti slope and its marginal area developed paleohighs and formed multiple sets of reservoir-cap combinations, leading to migration and accumulation of hydrocarbons during various periods (Li, 2009; Zhao, 2012; Tian, 2013). However, this exploration has not achieved a breakthrough in the past 20 years. Also, early research and exploration of the Maigaiti slope were focused on the Carboniferous system as a major target layer (Zheng, 1995; He et al., 1999; Zhou et al., 2006; Yang et al., 2007). No studies on the formation and evolutionary mechanisms of the deep paleokarst reservoirs in the Ordovician weathered crust have been reported, which has resulted in a lack of knowledge of this area's changing patterns. By using Ordovician carbonatite rocks and paleokarst fissure/cave-filling calcite as study subjects in addition to carbon-oxygen and strontium isotopes and trace element techniques, this study attempts to examine the development of paleokarst reservoirs and the larger paleoenvironment to provide geochemical evidence for the exploration and development of karst reservoirs.

2 Study area and methods

2.1 Study area

The Maigaiti slope is located in the southern Bachu uplift in the Tarim Basin (Figure 1) and extends in a northwest-southeast direction with an area of approximately $5 \times 104 \text{ km}^2$. The Maigaiti slope is a foreland slope that was developed after multistage tectonic movement in a foreland basin southwest of the Tarim Basin with a regional southward-dipping shape. The current Maigaiti slope has an overall structure of large-scale broad and gentle slopes inclined to the south. Oil and gas resources in the foreland basin southwest of the Tarim Basin are abundant (Jin et al., 2006), although progress has been limited due to the difficulty in exploration. Thus far, the Bashituopu oil/gas field with the Carboniferous system as the production layer in the west of the Maigaiti slope and the Hetianhe gas field with the Ordovician carbonatite rock-containing buried hill and Carboniferous system as the production layer in the Mazhatage tectonic belt on the northern border of the eastern Maigaiti slope have been identified.

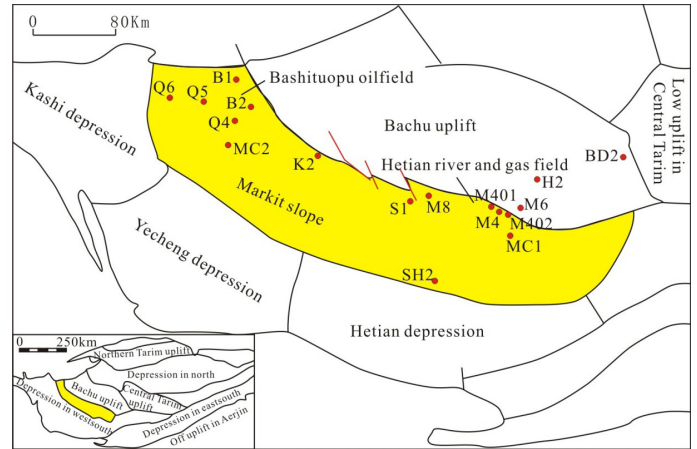


Figure 1. Location map of the Maigaiti slope in the Tarim Basin

Well-drilling exploration has revealed the absence of the Middle Ordovician Yijianfang and Upper Ordovician Tumuxiuke formations in the central Tarim uplift between the Mid-Lower Ordovician Yingshan and the Upper Ordovician Lianglitage formations of the Bachu uplift (Yang et al., 2011). Besides, the development of a large area of Yingshan Formation weathered crust and M2 near the Maigaiti slope was drilled within the set of stratigraphic unconformity. The South Bachu area west of the SH2 well and wells to the south of the Bachu County-GD3 well all lacked upper Ordovician Sangtamu Formation mudstone, and the Lianglitage Formation was missing up to the south of the J1 well-K2 well-S1 well of the Maigaiti slope. The Yingshan Formation emerged on the top of the Ordovician development in the northwest to the southwest of the paleo uplift, and an extensive distribution of the weathered crust of Ordovician carbonatite rocks is noted. The development zone is about 430 km long and about 210 km wide, and the area is about $9.1 \times 104 \text{ km}^2$ (Figure 2).

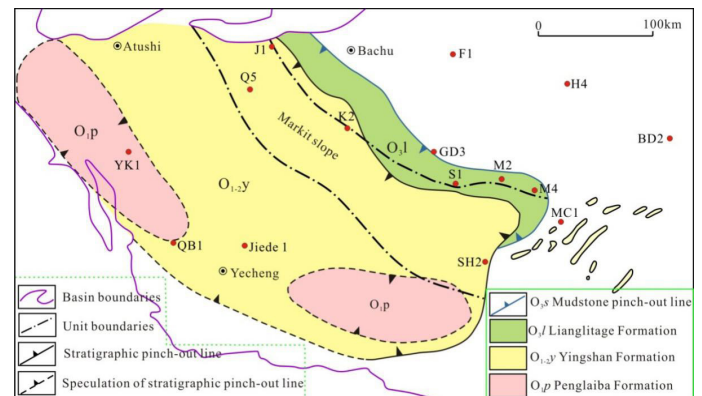


Figure 2. Distribution map of the Maigaiti slope and the periphery of the Ordovician weathered crust

The northwest-banded distribution of weathered crust in the Upper Ordovician Lianglitage Formation is developed south of the Upper Ordovician Sangtamu Formation mudstone pinch-out line. The strata are mainly based on the platform facies of mud and limestone, and the thickness of the biological debris is more than 400 m. The Maigaiti slope is based on the weathered crust of the Middle and Lower Ordovician Yingshan formations. The northeast locality exhibits the weathered crust of the Lianglitage Formation. The western Yingshan Formation is based on the open platform of the low-energy micrite development phase and has a lithological density. The eastern Yingshan Formation's top surface mainly presents high-energy particle and dust-grain limestone beach facies, mainly based on a thick layer of sparry calcarenite and micrite interbeds.

This layer becomes thinner to the south of the paleo uplift and includes two pieces of the Yingshan Formation lacking in the previous zone. The Penglaiba Formation dolomite and calcite-dolomite are exposed (Figure 3).

(a) M401 well, O_3^f , 2242.0 m, sparry bioclastic limestone, transmission of single polarization, 10×2.5 ; (b) K1 well, O_3^f , 3283.56 m, mud micrite, transmission orthogonal polarization, 10×10 ; (c) LN1 well, O_3^f , 4728 m, microcrystalline sand-dust bioclastic limestone, transmission of single polarization, 10×10 ; (d) M2 well, O_{1-2}^y , 2377.5 m, powder fine-grained dolostone, transmission orthogonal polarization, 10×10 ; (e) M4 well, O_{1-2}^y , 2021.6 m, microcrystalline limestone, transmission orthogonal polarization, 10×10 ; (f) K2 well, 3821.95 m, O_{1-2}^y , fine-grain dolostone transmission orthogonal polarization, 10×2.5 .

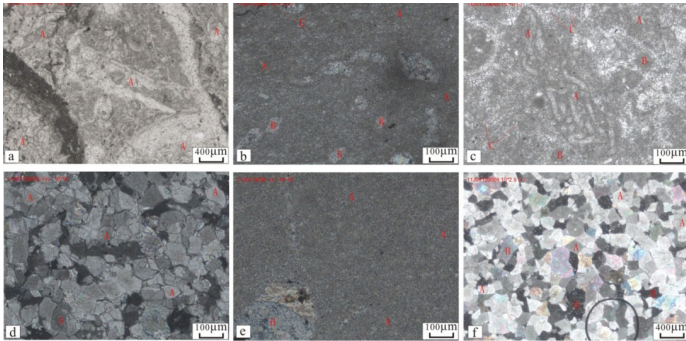


Figure 3. Petrological characteristics of Ordovician carbonatite rocks of Maigaiti slope

2.2. Samples and experiment

The trace element sampling layer is the Lower Middle Ordovician Yingshan Formation (O_{1-2}^y), from which a total of 37 rock-seam and karst cave infill pieces were collected including 12 pieces of seam-hole bedrock (limestone), 12 pieces of mechanical sand-shale infills, 8 pieces of chemical calcite infills, and 5 pieces of karst cave in karst breccia (limestone breccia). Testing and analysis were completed in the Karst Geological Resources and Environmental Supervision and Inspection Center of the Ministry of Land and Resources by using Axios X-ray fluorescence spectrometry to conduct measurements of trace elements in the sample. The measurement instrument is 2000 DV with a detection limit of 0.001%, an error of 0.002%, and measurement according to the Y/T05-1996 inductively coupled plasma (ICP) spectrum method.

In the analysis of carbon and oxygen isotopes, nine samples of the Ordovician bedrock drilling core and 45 samples of the paleokarst cave-filling calcite were used. Testing and analysis were completed in the Karst Geological Resources and Environmental Supervision and Inspection Center of the Ministry of Land and Resources. The accuracy of analysis adopted the Chinese national carbonate standards (GBW04405, GBW04406, GBW04416, and GBW04417) for correction and the level of carbon isotopes in carbonatite (NBS18) for monitoring. The standard deviation of $\delta^{13}C$ and $\delta^{18}O$ was 0.005‰ and 0.07‰, respectively. The test results are given in the Pee Dee Belemnite (PDB) standard; the test temperature and humidity were 25 °C and 60%, respectively.

In the Sr isotope analysis, 21 samples were obtained from the M2 well of the Lianglitage Formation of the Liang second section to the Liang fifth section (O_3^{f-5}) bedrock and 2 were obtained from the Lower Yingshan Formation (O_{1-2}^y) bedrock; both are composed of limestone. The tests were performed in the Wuhan Geological Survey Center’s Isotope Superclean Laboratory of the China Geological Survey. The instrument used is a MAT261 thermal ionization mass spectrometer with a testing standard obtained from a standard sample of the National Bureau of Standards of the United States. The measured value error (2σ) of $^{87}Sr/^{86}Sr$ was less than 0.006‰. The chemical process adopted the general international standard, and separation and purification were performed by using a cation-exchange column following that performed in the sample solution. The entire process blank was $<5 \times 10^{-10}g$, the laboratory temperature was 22 °C, and the humidity was 50%.

Sample collection of Ordovician limestone and the paleokarst seam-

hole filling calcite was performed at a buried depth range of 2023.32 – 4698.30 m in the Yingshan (O_{1-2}^y) and Lianglitage formation (O_3^f) strata, and the sampling wells were distributed in the entire zone. A limited number of drilling cores was available because the exploration zone is new. Samples were collected on three separate occasions.

3 Results and analysis

3.1 Geochemical characteristics of Sr isotope

Because of the unique nature of the Sr isotope, it is widely applied in such fields as marine stratigraphic dating (Dingle et al., 1997; Denison et al., 1998), global geological event comparisons (Crame et al., 1999; Jiang et al., 2001), diagenesis fluid research (Huang et al., 2004; Roger et al., 2004), and paleoclimatic and ancient marine environmental analyses (Huang et al., 2002; Shi et al., 2005; Liu and Ji 2008). However, the application of the Sr isotope in the study of paleokarst reservoirs is a new concept. Few reports on this topic are available (Wen 2014; Zheng et al. 2008); only diagenesis effects appear in published reports that applied the trace elements of Sr and $^{87}Sr/^{86}Sr$ values (Montanez, 1994; Banner, 1995; Heydari, 2003).

The Sr isotope analysis results (Table 1) in 23 samples of the M2 well in the Lianglitage Formation marine carbonatite rocks showed that the $^{87}Sr/^{86}Sr$ sample value was within the range of 0.70851–0.70913; the average value was 0.70877, and the average error was around 4.71×10^{-5} . Because of old-to-new stratum transitioning, the Sr isotope ratio displayed an overall decreasing trend (Table 1, Figure 4), and its value was within the range of the Ordovician $^{87}Sr/^{86}Sr$ (0.7078–0.7092) from Shields et al. (2003) of brachiopod shell animal fossils and the ratio range obtained by Burke et al. (1982) and Veizer et al. (1999). The $^{87}Sr/^{86}Sr$ of this sample was higher than global normal of the marine carbonatite rocks in the Late Ordovician, which was 0.7078–0.7082 (Denison et al., 1998; McArthur et al., 2001). However, the $^{87}Sr/^{86}Sr$ value reported by Liu et al. (2012) in six wells in the central Tarim area Lianglitage Formation was 0.708136–0.719936, and the average value was 0.7099. The $^{87}Sr/^{86}Sr$ value of the Lianglitage Formation of Bachu area reported by Zhao et al. (2013) was 0.708032–0.708759, and the average value was 0.7099. The Late Ordovician $^{87}Sr/^{86}Sr$ average value of the central Tarim GZ4 well obtained by Huang et al. (2006) was 0.709173. The Late Ordovician Sr isotopic ratio of most areas of the Tarim Basin is larger than the global maximum range of normal Sr isotopes of marine carbonatite rocks, at 0.7082. This result is relevant to the higher $^{87}Sr/^{86}Sr$ ratio of seawater caused by the Lianglitage Formation of terrigenous material entering the basin during the deposition period (Zheng et al., 2008).

Table 1. Analysis results of the Sr isotope of carbonatite rocks in 23 samples obtained from the study area.

Location	Sample number	$^{87}Sr / ^{86}Sr$	$2\sigma\pm$	Location	Sample number	$^{87}Sr / ^{86}Sr$	$2\sigma\pm$
O_3^f	S1	0.708 78	0.000 03	O_3^f	S13	0.708 80	0.000 06
O_3^f	S2	0.708 85	0.000 06	O_3^f	S14	0.708 88	0.000 05
O_3^f	S3	0.708 76	0.000 02	O_3^f	S15	0.708 75	0.000 06
O_3^f	S4	0.708 69	0.000 01	O_3^f	S16	0.708 51	0.000 05
O_3^f	S5	0.708 67	0.000 08	O_3^f	S17	0.708 56	0.000 02
O_3^f	S6	0.708 79	0.000 02	O_3^f	S18	0.708 82	0.000 04
O_3^f	S7	0.708 56	0.000 03	O_3^f	S19	0.709 01	0.000 07
O_3^f	S8	0.708 65	0.000 02	O_3^f	S20	0.708 87	0.000 07
O_3^f	S9	0.708 60	0.000 04	O_3^f	S21	0.709 13	0.000 02
O_3^f	S10	0.708 72	0.000 05	O_{1-2}^y	S22	0.709 00	0.000 14
O_3^f	S11	0.708 87	0.000 01	O_{1-2}^y	S23	0.708 92	0.000 05
O_3^f	S12	0.708 76	0.000 08				

3.2 Geochemical characteristics of carbon and oxygen isotopes

The geochemical characteristics of carbon and oxygen isotopes in the paleokarst have great significance in analysis of the origin and forming conditions of carbonatite sedimentary environment, diagenesis, and cementation filling (Zhang et al. 2011). Different types of karst encountered different fluidic environments during the formation process; thus, the use of a geochemical method could better identify and distinguish various types of corrosion. The carbon and oxygen isotopic characteristics of carbonatite rocks and karst cave-filling calcite in Markit slope Ordovician are shown in Table 2.

Table 2. Carbon and oxygen isotopic characteristics of karst cave-filling calcite and bedrock.

Locat ion	Positi on	Depth	Sample	$\delta^{13}\text{C}_{\text{PDB}}\text{‰}$	$\delta^{18}\text{O}_{\text{PDB}}\text{‰}$	Locati on	Positi on	Depth	Sample	$\delta^{13}\text{C}_{\text{V-PDB}}\text{‰}$	$\delta^{18}\text{O}_{\text{V-PDB}}\text{‰}$
J1	O ₁₋₂₃ ¹	4587.28	Calcite	-0.62	-10.51	M2	O ₁₋₂₃ ²	2377.5	Calcite	-3.36	-11.24
K1	O ₃ ¹	3125.06	Calcite	0.53	-8.99	M3	O ₃ ¹	2515.95	Calcite	-0.52	-13.01
K1	O ₃ ¹	3283.56	Calcite	-1.97	-14.49	M4	O ₁₋₂₃ ¹	2028.95	Calcite	-2.99	-9.75
K2	O ₃ ¹	3410.10	Calcite	0.67	-10.42	M4	O ₁ ¹	2611.20	Calcite	-2.47	-7.75
LS1	O ₃ ¹	4070.74	Calcite	2.02	-7.61	M5	O ₃ ¹	2234.00	Calcite	0.8	-7.73
LN1	O ₃ ¹	4636.71	Calcite	0.65	-7.58	M5-1	O ₃ ¹	2239.89	Calcite	-0.89	-8.69
GD1	O ₁ ¹	2544.00	Calcite	-5.02	-8.06	M7	O ₃ ¹	2327.96	Calcite	1.07	-7.83
GD2	O ₃ ¹	2681.00	Calcite	0.6	-9.97	M401	O ₃ ¹	2275.53	Calcite	0.75	-12.62
GD3	O ₃ ¹	2251.00	Calcite	0.8	-7.24	M401	O ₃ ¹	2308.75	Calcite	1.58	-8.22
H3	O ₁₋₂₃ ¹	4526.45	Calcite	-1.29	-15.53	M402	O ₃ ¹	2320.31	Calcite	0.39	-9.28
M2	O ₃ ¹	2619.20	Calcite	0.03	-8.99	MC1	O ₁₋₂₃ ²	4476.09	Calcite	-3.81	-9.23
M2	O ₁₋₂₃ ¹	2025.00	Calcite	-2.06	-6.21	TN1	O ₃ ¹	4698.3	Calcite	3.06	-9.95
GD1	O ₁ ¹	2513.23	Calcite	-0.4	-10.76	LN1	O ₃ ¹	4697.73	Calcite	-0.23	-8.79
GD2	O ₃ ¹	2785.65	Calcite	0.08	-8.74	M5	O ₃ ¹	2252.45	Calcite	-1.76	-11.11
GD3	O ₃ ¹	2234.76	Calcite	-0.13	-6.29	M5-1	O ₃ ¹	2241.95	Calcite	-1.32	-9.01
H3	O ₁₋₂₃ ¹	4544.36	Calcite	0	-7.29	M7	O ₃ ¹	2354.45	Calcite	-1.6	-9.28
M2	O ₃ ¹	2625.75	Calcite	0.6	-5.76	M401	O ₃ ¹	2288.34	Calcite	-0.09	-8.72
M2	O ₁₋₂₃ ¹	2034.35	Calcite	-0.53	-8.28	M401	O ₃ ¹	2319.82	Calcite	-1.39	-8.85
M2	O ₁₋₂₃ ¹	2379.93	Calcite	0.58	-8.6	MC1	O ₁₋₂₃ ²	4479.64	Bedrock	-0.52	-7.57
M3	O ₃ ¹	2601.32	Calcite	0.76	-11.83	TN1	O ₃ ¹	4678.95	Bedrock	-0.78	-6.37
M4	O ₁₋₂₃ ¹	2037.95	Calcite	0.15	-12.41	GD1	O ₁ ¹	2554.37	Bedrock	0.43	-6.14
M4	O ₁ ¹	2625.24	Calcite	0.33	-7.61	GD2	O ₃ ¹	2676.28	Bedrock	0.56	-6.04
J1	O ₁₋₂₃ ¹	4596.23	Calcite	1.23	-3.56	GD3	O ₃ ¹	2266.35	Bedrock	0.27	-7.38
K1	O ₃ ¹	3212.56	Calcite	0.98	-6.75	H3	O ₁₋₂₃ ¹	4543.10	Bedrock	0.02	-5.94
K1	O ₃ ¹	3303.25	Calcite	0.11	-8.92	M2	O ₃ ¹	2631.09	Bedrock	-0.38	-7.16
K2	O ₃ ¹	3442.75	Calcite	0.09	-9.11	M2	O ₁₋₂₃ ¹	2023.32	Bedrock	-0.86	-6.81
LS1	O ₃ ¹	4069.19	Calcite	-0.14	-8.63	M2	O ₁₋₂₃ ²	2382.00	Bedrock	-0.83	-6.63

Numerous test results using PDB as the standard showed that most modern marine inorganic carbonatite $\delta^{13}\text{C}$ values are close to 0‰ (Liu et al., 2004); the $\delta^{18}\text{O}$ values are also close to 0‰ (Gu, 2000). According to the sample test results (Table 2, Figure 3), the $\delta^{13}\text{C}$ and $\delta^{18}\text{O}$ of carbonatite karst cave filling in the Markit slope Ordovician deviated significantly from these values. The alteration span was large; the $\delta^{13}\text{C}$ (PDB) values were from 3.06‰ to -5.02‰, and the average value was -0.3‰; the $\delta^{18}\text{O}$ values were between -4.56‰ and -15.53‰, and the

average value was -8.74‰. These values are similar to those of the carbon and oxygen isotope samples in Tahe oilfield Ordovician karst cave-filling, in which the average values of $\delta^{13}\text{C}$ and $\delta^{18}\text{O}$ from 21 data points were -0.807‰ and -9.14‰, respectively (Liu et al., 2008). These results exhibited no significant differences from those of the central Tarim area TZ12 wells, in which the average values of $\delta^{13}\text{C}$ and $\delta^{18}\text{O}$ from four data points were -1.08‰ and -7.05‰, respectively (Jiang, 2002). Moreover, they are similar to the average values of $\delta^{13}\text{C}$ and $\delta^{18}\text{O}$ in the eastern Lungu area, which from 25 data points were -1.40‰ and -10.74‰, respectively (Zhang, 2015). The phenomenon of individual points shifting to the two ends was noted. The $\delta^{18}\text{O}$ values in carbonatite bedrock were between -7.57‰ and -5.94‰, and the $\delta^{13}\text{C}$ values were from -0.86‰ to 0.56‰.

3.3 Geochemical characteristics of trace elements

The test results (Table 3) show that the average range of Sr content in all types of bedrock and karst cave-filling calcite and karst breccia was between 132.564×10^{-6} and 183.683×10^{-6} , and the average content of Sr in karst cave-filling sand-shale was 77.219×10^{-6} . Overall, the Sr content values were less than the lower limit of the Sr content value (200×10^{-6}) in the accurate representation of homogenized seawater samples proposed by Derry et al. (1989). The average Sr content value that best represents seawater micrite was only 183.683×10^{-6} , which indicates leaching and dissolving of carbonatite rock by meteoric water.

The mean value of Fe content ($1232 \times 10^{-6} - 5651.8 \times 10^{-6}$) in the karst cave-filling materials such as karst breccia, sand-mud rocks, and filling calcite was larger than that in bedrock ($385 \times 10^{-6} - 669.9 \times 10^{-6}$). In addition, the Mn element content in the karst cave-filling calcite and karst breccia was higher than that in the bedrock, indicating that they were formed through complete open meteoric water karstification conditions (Huang et al., 2006; Huang et al., 2008) because the respective contents of Sr and Mn are lower and higher in meteoric water than those in seawater (Walter et al., 2000; Huang et al., 2008). Also, under oxidizing conditions, Fe and Mn in high states would be leached and filled by meteoric water in the matrix between the karst breccia fragments, and their contents would be very high (Wen, 2014).

Because Sr and Ba are alkaline earth metals with similar chemical properties, they were separated owing to their geochemical behaviors in various environments. Usually, terrigenous sediments are relatively rich in Ba and poor in Sr, whereas marine sediments are relatively rich in Sr and poor in Ba. Thus, researchers have analyzed the changes in carbonatite rock salinity during the formation process by using the Sr/Ba ratio (He et al., 2004; Huang, 1990; Tao et al., 2009). Further, a Sr/Ba ratio greater than 1 indicates a marine sedimentary environment, whereas that less than 1 indicates a freshwater sedimentary environment. The Sr/Ba ratios for the three types of infills in the Ordovician karst cave in the Markit slope were considerably less than 1. This confirms that their formations are related to fresh water and proves the existence of ancient weathered crust karstification (Li et al., 2009).

Also, multivariate statistical methods used to handle large amounts of data can summarize the trace element data according to the relationships of quantity, behavior, and characteristics and can provide a series of trends to draw a reasonable inference (Fan et al., 1999). Correlation analysis was conducted on CaO and SiO₂, which reflected the sand-shale rock composition and trace elements (Table 4). The correlation coefficient of CaO and SiO₂ was -0.991, illustrating that both were highly irrelevant; those of SiO₂, P, Cr, Ba, Co, and Ni were greater than 0.8, indicating that similar to SiO₂, the trace elements of P, Cr, Ba, Co, and Ni were enriched in sandstone and mudstone. The correlation coefficients of Zn, Pb, and Cd as trace elements were larger than 0.8, although the negative correlation was noted with P, Cr, Ba, Co, and Ni. These results imply that the enrichment mechanism of Zn, Cd, and Pb differed from that of SiO₂.

The mechanical filling in sand-shale was compared with that of bedrock. The former had a high combination of trace elements including P, Cr, Ba, Co, and Ni, indicating that its source was mainly exposed or shallow burial conditions in which sand-shale rich in P, Cr, Ba, Co, and Ni trace elements was weathered when flowing water entered the karst cave space. However, the Cu content in sand-shale reached 16.291 possibly owing to the burial conditions. The contents of heavy metal trace elements that easily migrated within compaction-released water or hot water in the karst cave was significantly higher than that in bedrock, even forming compounds with S. The correlation of calcite and bedrock was

relatively high, although the calcite was rich in Mn and poor in Sr. This indicates that the calcite formed in a meteoric water environment. The comparison between collapse breccia and bedrock revealed that although higher contents of P, Cr, Ba, Co, and Ni occurred in the collapse breccia,

they were lower than those in the sand–shale filling. The average value of Sr was lower than that in the bedrock and higher than that in the sand–shale filling, which reflects the cave development mode of cementation of collapsed bedrock roof by calcium shale.

Table 3. Trace element contents of various rock types and filling materials.

Karst structure	Lithology	Sample number/block	Average values of trace element contents/10 ⁶														
			Fe	Mn	Sr	Ba	P	As	Cd	Co	Cr	Cu	Ni	Pb	Zn	Mo	Sr / Ba
Bedrock	Muddy limestone	9	669.9	95.586	183.683	18.928	61.211	6.456	0.500	2.978	0.106	6.500	4.633	100.656	308.944	0.411	10.23
	Ash rock	3	385	141.576	155.231	9.67	55.800	6.700	0.200	0.800	0.050	6.100	4.000	77.200	78.100	0.250	16.05
Karst cave	Sand–shale	12	5651.8	65.385	77.219	251.635	501.718	6.173	0.114	26.427	58.227	16.291	29.627	53.845	48.827	1.336	0.32
Filling materials	Calcite	8	1232	355.984	136.587	268.79	73.567	6.200	0.167	4.567	2.367	8.067	6.700	81.767	83.133	0.250	0.51
	Karst rock	5	3388	348.638	132.564	290.9	183.400	4.700	0.100	4.300	19.700	8.300	10.000	62.900	29.500	0.250	0.45

Table 4. Analysis of correlation between different elements

	$\omega(\text{SiO}_2)$	$\omega(\text{CaO})$	$\omega(\text{P})$	$\omega(\text{Mn})$	$\omega(\text{As})$	$\omega(\text{Ba})$	$\omega(\text{Cd})$	$\omega(\text{Co})$	$\omega(\text{Cr})$	$\omega(\text{Cu})$	$\omega(\text{Ni})$	$\omega(\text{Pb})$	$\omega(\text{Sr})$	$\omega(\text{Zn})$	$\omega(\text{Mo})$
$\omega(\text{SiO}_2)$	1.000														
$\omega(\text{CaO})$	-0.991	1.000													
$\omega(\text{P})$	0.867	-0.846	1.000												
$\omega(\text{Mn})$	-0.367	0.308	-0.319	1.000											
$\omega(\text{As})$	0.002	-0.027	-0.087	-0.261	1.000										
$\omega(\text{Ba})$	0.828	-0.861	0.851	-0.158	-0.031	1.000									
$\omega(\text{Cd})$	-0.442	0.443	-0.381	-0.100	0.041	-0.418	1.000								
$\omega(\text{Co})$	0.901	-0.887	0.830	-0.407	0.168	0.725	-0.332	1.000							
$\omega(\text{Cr})$	0.936	-0.926	0.913	-0.325	0.024	0.887	-0.427	0.859	1.000						
$\omega(\text{Cu})$	0.710	-0.723	0.501	-0.262	0.517	0.615	-0.258	0.661	0.752	1.000					
$\omega(\text{Ni})$	0.921	-0.914	0.853	-0.408	0.209	0.823	-0.399	0.939	0.927	0.772	1.000				
$\omega(\text{Pb})$	-0.659	0.651	-0.577	0.121	0.090	-0.571	0.864	-0.537	-0.614	-0.367	-0.592	1.000			
$\omega(\text{Sr})$	-0.792	0.746	-0.698	0.192	0.060	-0.608	0.441	-0.699	-0.773	-0.625	-0.738	0.602	1.000		
$\omega(\text{Zn})$	-0.425	0.423	-0.374	-0.111	0.078	-0.401	0.995	-0.307	-0.415	-0.230	-0.376	0.877	0.446	1.000	
$\omega(\text{Mo})$	0.580	-0.585	0.491	-0.268	-0.074	0.439	-0.249	0.559	0.380	0.210	0.512	-0.420	-0.338	-0.233	1.000

4. Discussion

4.1. Environmental and geological significance of Sr isotope

The Sr isotope ratio is a sensitive indicator of sea level change. A geological period including a rise and fall of the sea level would cause changes in the sedimentary environment that are recorded in sedimentary carbonatite rocks in the same period; thus, changes in the Sr isotopic ratio in a rock can reflect the geological period of sea level

settlement and ancient marine environment characteristics (Li and Guan, 2001). With an increase in sea level, the weathering rate is reduced, surface runoff decreases, and surface rock weathering and denudation decreases. Moreover, a relatively small amount of Sr isotopes enter the oceans, resulting in a decrease in the marine Sr isotope ratio. However, a decrease in sea level leads to an increase in the marine Sr isotope ratio. Therefore, sea-level fluctuation and the ⁸⁷Sr/⁸⁶Sr value change is negatively correlated (Yan et al., 2005).

The isotope test results of M2 well carbonatite rock Sr (Figure 4) indicated many high $^{87}\text{Sr}/^{86}\text{Sr}$ values in the fifth Liang section at 1935–1960 m. The highest value, 0.70913, occurred in the middle of this section and may correspond to the closure of the southern Tianshan ocean in this period and the entry of large amounts of terrigenous detrital materials (Zheng et al., 2008). Between the end of the fifth Liang section (O_3I^5) and the fourth Liang section (O_3I^4), sea levels underwent a slight decline and then increased at a relatively rapid rate, marked by the minimum $^{87}\text{Sr}/^{86}\text{Sr}$ ratio of 0.70851. This process may have been influenced by the Keping uplift, which offsets the sea level rise to a certain extent (Zhao, 2013).

Between the fourth Liang section (O_3I^4) and the third Liang section (O_3I^3), the sedimentary environment changed to foreslope facies. The lithology was varied from nuclear-shaped limestone to marl and micritic limestone, and the stratigraphic thickness changed from thin to thick layers. Moreover, the $^{87}\text{Sr}/^{86}\text{Sr}$ values reached a low value of 0.70856, and the sea level rose significantly. During the period of the second Liang depositions (O_3I^2), sea level began to decline gradually, and the sedimentary environment changed to platform sediment with an open platform.

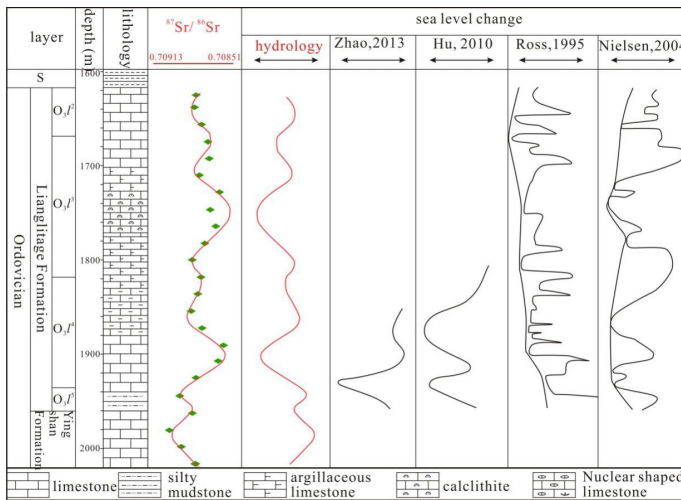


Figure 4. Comparison of sea level changes among the Markit and Bachu, Keping, Laurentia, and Baltica continents.

In their global Sr isotope study, McArthur et al. (2001) used locally weighted scatterplot smoothing (LOWESS) to establish a 0–509 Ma Sr isotope fitting curve; their results created a complete Sr isotope evolution curves at that time (Huang et al., 2004) (Figure 5a). The Sr isotopic evolution curve in the Late Ordovician Lianglitage Formation sedimentary period was established by combining the Sr isotope data of Bachu reported by Zhao, 2013 and that of Central Tarim reported by Liu et al. (2012) (Figure 5b). The Sr isotope ratios determined from the global curve fitting in the Late Ordovician ($455 \times 10^6\text{a} - 445 \times 10^6\text{a}$) seawater displayed a monotonically decreasing trend with forwarding time whereas after $445 \times 10^6\text{a}$, the $^{87}\text{Sr}/^{86}\text{Sr}$ ratio generally presented an upward curve trend, which had good consistency with the deposition from the sea level change of the Lianglitage Formation. This result reflects that the sea level change of the Markit slope had a relatively good correlation with Bachu (Zhao, 2013), Central Tarim (Liu et al., 2012), Laurentia (Ross and Ross, 1995), and the Baltoscandian paleocontinent in the Late Ordovician (Figure 5).

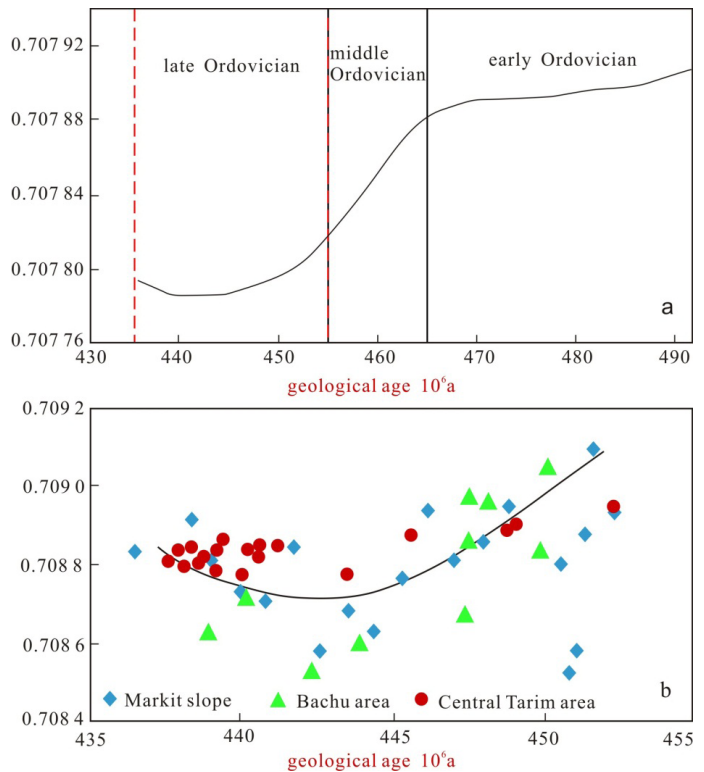


Figure 5. Evolution trend of Sr isotopes in the Ordovician marine strata and evolution curves of Sr isotopes in the Late Ordovician Lianglitage Formation.

For the carbon isotopes, carbon is stored in two large carbon pools including organic carbon (carbon reduction) and inorganic carbon (carbon dioxide). The average value difference of $\delta^{13}\text{C}$ between these two is about 25%. Therefore, of the factors affecting carbon isotopes in marine carbonatite rocks, oxidation and relative burial volume of organic carbon was the most important at that time (Huang, 1997; Wang et al., 2009). When the relative burial volume of organic carbon was higher than the amount of oxidation, more ^{12}C entered the organic carbon, which made the $\delta^{13}\text{C}$ value of the marine carbonatite rocks in the same period move toward the positive direction. Also, the increasing salinity of the deposition in the water medium would have caused increases in carbonatite $\delta^{13}\text{C}$ (Clayton and Degens, 1959; Keith and Weber, 1964); atmospheric precipitation and terrestrial freshwater injection would have caused $\delta^{13}\text{C}$ value decreases. Oxygen isotopes are greatly influenced by the temperature and the concentration of the medium. Moreover, the $\delta^{18}\text{O}$ value will significantly increase with an increase in water media salinity in the sedimentary environment and a strengthening in evaporation (Clayton and Degens, 1959; Keith and Weber, 1964).

The $\delta^{18}\text{O}$ values of calcite and bedrock fill in the Markit slope karst cave had negative characteristics such that the span of $\delta^{13}\text{C}$ values was significant. This result is related to the Ordovician surface uplift, the overall open environment, meteoric water eluviation (Land, 1980; Rosen et al., 1989; Gasparrini et al., 2006) of widespread $\delta^{13}\text{C}$, and all $\delta^{16}\text{O}$ of atmospheric CO_3^{2-} sources (Veizer et al., 1999; Azmy et al., 2009).

The relationship diagram of $\delta^{13}\text{C}-\delta^{18}\text{O}$ (Figure 6) indicates that the filling materials in the Markit slope Ordovician carbonatite fracture cave can be divided into four classes indicating differences in formation's environment (Table 5).

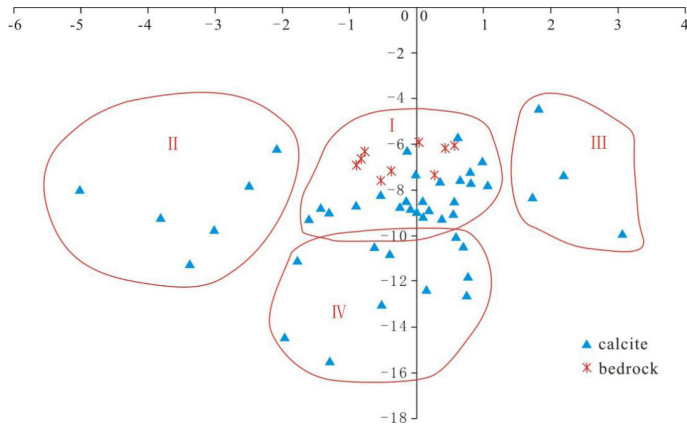


Figure 6. The cross-diagram of carbon and oxygen isotopes for filling materials in the Markit slope Ordovician karst cave system.

Table 5. Response characteristics of karst development stage and filling environment

Development stage	Formation environment	Isotope features	
		δ ¹³ C(PDB)‰	δ ¹⁸ O(PDB)‰
I	Marine environment during syndiagenesis	-1.60 to -1.07	-9.28 to -5.76
II	Freshwater environment	-5.02 to -2.06	-11.24 to -6.21
III	Shallow buried environment	1.58 to 3.06	-9.95 to -4.56
IV	Deep buried high-temperature environment	-1.97 to 0.76	-15.53 to -9.97

Class I is the marine environment during the syndiagenetic stage, which reflects the isotope characteristics of early paleo-karstification environment filling. The δ¹⁸O of the karst cave calcite was -9.28‰ to -5.76‰, and the δ¹³C was -1.60‰ to -1.07‰. The distribution ranges were similar to those of the limestone background value area. Individual points drifted toward both ends, indicating that the oxygen and carbon isotope compositions of the fractures and cave calcite were controlled mainly by δ¹³C and δ¹⁸O in the original rock, followed by subsequent freshwater leaching and transformation (Land et al., 1980; Rosen et al., 1989). The values for some points of the δ¹³C displayed negative bias.

Class II is weathered crust exposed in a karst freshwater filling environment. The δ¹⁸O values of the filling calcite were -11.24‰ to -6.21‰, and δ¹³C was between -5.02‰ and -2.06‰. Owing to the influence of fresh atmospheric water (Gasparini et al., 2006), the δ¹³C values were apparently smaller than the bedrock carbon isotope values, which were formed in the open environment.

Class III is a shallow buried karst environment. The δ¹⁸O values of the karst cave filling calcite were between -9.95‰ and -4.56‰, and the δ¹³C values were from 1.58‰ to 3.06‰. The δ¹³C showed obvious positive bias likely caused by decomposition and methanation (CH₄) of organic matter caused by methane bacteria.

CH₄ formed from biochemical processes was rich in d¹²C, whereas the CO₂ had abundant d¹³C. Because CO₂ released during the reaction of methane bacteria fermentation participated in the process of karstification and sedimentary filling, the sedimentary filling was rich in d¹³C and presented higher positive values.

Class IV is a deep-burial high-temperature environment. The δ¹⁸O in calcite was between -15.53‰ and -9.97‰, and the δ¹⁸O values were obviously negatively biased, reflecting the clear relationship between the formation of calcite filling and hydrothermal activity. Owing to the influence of heat loss in the transformation of deep δ¹⁸O in the burial stage (Tritlla et al., 2001; Lavoie and Chi,

2006), the δ¹⁸O values presented negative bias. Also, the diagenesis stage was a period of organic matter thermal maturation. A large amount of organic acid-based compaction-released water caused dissolution and alteration in the carbonatite rocks and early-stage fracture calcite. Moreover, it led to organic carbon injection, which resulted in δ¹³C loss and negative bias (Boni et al., 2000; Azmy et al., 2009).

4.3 Geoenvironmental significance of trace elements

The element content in a mineral is attributed mainly to the concentration and kinetic effect of that element in a precipitation solution (Huang, 1990). Because seawater is an environment of low Mn and Fe, the contents of these elements are far less than those in fresh water. According to the characteristics of trace elements in all types of bedrock and infill examined in this study, paleokarst fractured reservoirs in the Markit slope Ordovician Yingshan Formation can be divided into the following three paleoenvironment hydrological conditions:

(1) Active oxidizability freshwater environment in the seepage-active hyporheic zone. During the karst process, surface clay or bauxite enters the underground karst fissure caves with meteoric water, which results in enrichment of Fe, K, Ti, P, Cr, Ba, Co, and Ni trace elements in the sandstone and mudstone in the cave. Also, cave collapsing breccia retains the characteristics of trace elements in the bedrock, although shale calcium cementation retains traces of the meteoric effect.

(2) Subcurrent stagnant freshwater environment. The calcite precipitates easily owing to the low flowability of the fresh water. Because the main components originate from the bedrock, they are affected by meteoric water, resulting in loss of Sr, and enrichment of Fe and Mn.

(3) Burial environment. Through changes in temperature and pressure, compaction-released water is formed and flows. This fact leads to migration and depletion of elements, particularly in the enrichment of heavy metals such as Zn, Cd, Pb, and Cu due to the involvement of S in the chemical reactions.

5 Conclusions

(1) Markit Slope is located in the Hetian paleo uplift, which belongs to three large paleo uplifts in the Tarim Basin. Exposed Ordovician carbonatite weathered crust is widely distributed and is particularly developed in Penglaiba Formation (O_{1p}), in which a cave-type karst carbonatite reservoir layer is developed. This area is ideal for the exploration and development of oil and gas in the Tarim Basin.

(2) The limestone in upper Ordovician Lianglitage Formation has high ⁸⁷Sr/⁸⁶Sr values, which shows good consistency with the ⁸⁷Sr/⁸⁶Sr values of the Keping and Central Tarim areas in the Tarim Basin of the same period. The Caledonian movement, in which a lot of clastic terrigenous was generated, might be the main reason for the increase in ⁸⁷Sr/⁸⁶Sr values. During the sedimentary period of the Lianglitage Formation, sea level fluctuation was frequent. However, an overall trend of increase followed by decrease was identified, which has good correlation with global sea level change.

(3) The δ¹⁸O values of filling calcite and bedrock in the Ordovician karst cave indicate negative bias. The δ¹³C values vary significantly at both ends, which presents an obvious deviation from the δ¹³C and δ¹⁸O values of normal marine carbonatite rock. However, these values are similar to those in the Tarim River, Central Tarim, and the ancient regions. Four different formation environments are indicated: class I, a marine environment during the syndiagenesis stage; class II, exposed weathered crust karst freshwater filling environment; class III, shallow buried karst environment; and class IV, deep-burial high-temperature environment.

(4) The analysis results of trace element for weathered crust bedrock and filling materials in the Ordovician Yingshan Formation (O_{1-2v}) showed that fissure/cave infills are enriched in Fe, and Mn and are depleted in Sr, which means that that filling materials were formed in a freshwater environment with low salinity. Moreover, the Sr/Ba ratio was markedly less than 1, confirming the existence of ancient weathered crust and the development of freshwater karst. According to the correlation analysis of trace elements in the bedrock and karst fissure/cave infills, the paleokarst system in the Yingshan Formation can be subdivided into three hydrological conditions of paleoenvironment: an active oxidizability freshwater environment in a seepage-active hyporheic zone; a sub-current stagnant freshwater environment; and a burial in a hydrothermal water environment.

Acknowledgments

This research was funded by the National Natural Science Foundation Project (41302122), National Key Basic Research Development (973 Program) Project (2011CB201001), and Public Welfare Industry Scientific Special Research (201211082) in Ministry of Land and Resources.

The authors express sincere thanks to Professor Wenqing Pan of the PetroChina Tarim Oilfield Exploration and Development Research Institute for helpful discussions about paleokarst fracture hole filling in a paleoenvironment and to the reviewers and editors who offered valuable advice for this paper.

References:

- Azmy, K., Knight, I., Lavoie, D. and Chi, G. (2009). Origin of dolomites in the Boat Harbour Formation, St. George Group, in western Newfoundland, Canada: Implications for porosity development. *Bulletin of Canadian Petroleum Geology*, 57(1), 81-104. DOI: [10.2113/gscpgbull.57.1.81](https://doi.org/10.2113/gscpgbull.57.1.81)
- Banner, J.L. (1995). Application of the trace element and isotope geochemistry of strontium to studies of carbonate diagenesis. *Sedimentology*, 42, 805-824. DOI: [10.1111/j.1365-3091.1995.tb00410.x](https://doi.org/10.1111/j.1365-3091.1995.tb00410.x)
- Boni, M., Parente, G., Bechstadt, T., Vivo, B.D. and Iannace, A. (2000). Hydrothermal dolomites in SW Sardinia (Italy): Evidence for a widespread late-Variscan fluid flow event. *Sedimentary Geology*, 131(3-4), 181-200.
- Burke, W. H., Denison, R.E., Hetherington, E.A., Koepnick, R.B., Nelson, H.F. and Otto, J.B. (1982). Variation of seawater $87\text{Sr}/86\text{Sr}$ throughout Phanerozoic time. *Geology*, 10(10), 516-519. DOI: [10.1130/0091](https://doi.org/10.1130/0091)
- Chen, X.S., Yi, W.X. and Lu, W.Z. (2004). The paleokarst reservoirs of oil/gas fields in China (in Chinese with English abstract). *Acta Sedimentologica Sinica*, 22(2), 244-253.
- Clayton, R.N. and Degens, E.T. (1959). Use of carbon isotope analyses of carbonates for differentiating fresh-water and marine sediments. *American Association of Petroleum Geologists Bulletin*, 43(4), 890-897.
- Crame, J.A., McArthur, J.M., Pirrie, D. and Riding, J.B. (1999). Strontium isotope correlation of the basal Maastrichtian Stage in Antarctica to the European and US biostratigraphic scheme. *Journal of the Geological Society*, 156, 5, 957-964. DOI: [10.1144/gsjgs.156.5.0957](https://doi.org/10.1144/gsjgs.156.5.0957)
- Denison, R.E., Kirkland, D.W. and Evans, R. (1998). Using strontium isotopes to determine the age and origin of gypsum and anhydrite beds. *Journal of Geology*, 106(1), 1-18. DOI: [10.1086/515996](https://doi.org/10.1086/515996)
- Derry, L.A., Keto, L.S., Jacobsen, S.B., Knoll, A.H. and Swett, K. (1989). Sr isotopic variations in Upper Proterozoic carbonates from Svalbard and East Greenland. *Geochimica et Cosmochimica Acta*, 53(9), 2331-2339. DOI: [10.1016/0016-7037\(89\)90355-4](https://doi.org/10.1016/0016-7037(89)90355-4)
- Dingle, R.V., McArthur, J.M. and Vroon, P. (1997). Oligocene and Pliocene interglacial events in the Antarctic Peninsula dated using strontium isotope stratigraphy. *Journal of the Geological Society*, 154(2), 257-264. DOI: [10.1144/gsjgs.154.2.0257](https://doi.org/10.1144/gsjgs.154.2.0257)
- Fan, X.L., Qiu, W.Y. and Bao, X.Y. (1999). The geological structure, formation of petroleum pools and hydrocarbon exploration in Lunnan-akekule area of the Tarim basin (in Chinese). *Petroleum Geology & Experiment*, 21(2), 132-136.
- Feng, J.L., Cao, J., Hu, K., Peng, X.Q., Chen, Y., Wang, Y.F. and Wang, M. (2013). Dissolution and its impacts on reservoir formation in moderately to deeply buried strata of mixed siliciclastic-carbonate sediments, northwestern Qaidam basin, Northwest China (in Chinese with English abstract). *Marine and Petroleum Geology*, 39(1), 124-137.
- Gasparrini, M., Bechstaedt, T. and Boni, M. (2006). Massive hydrothermal dolomites in the south western Cantabrian Zone (Spain) and their relation to the Late Variscan evolution. *Marine and Petroleum Geology*, 23(5), 543-568. DOI: [10.1016/j.marpetgeo.2006.05.003](https://doi.org/10.1016/j.marpetgeo.2006.05.003)
- Gu, J.Y. (2000). Characteristics and origin analysis of dolomite in lower Ordovician of Tarim Basin (in Chinese). *Xinjiang Petroleum Geology*, 21(2), 120-122.
- Guo, J.H. (1993). Burial Hill Palaeokarst and Its Controlled Reservoir Heterogeneity in Ordovician, Lunnan Region of Tarim Basin (in Chinese with English abstract). *Acta Sedimentologica Sinica*, 11(1), 56-64.
- He, D.F., Liu, S.B. Li, H.H. (1999): The big oil field exploration direction in Tarim basin: A case study of Maigaiti slope structure (in Chinese). *Petroleum Explorationist*, 4(2), 57-64.
- He, H., Peng, S.P. and Shao, L.Y. (2004). Trace Elements and Sedimentary Settings of Cambrian Ordovician Carbonates in Bachu Area, Tarim Basin (in Chinese with English abstract). *Xinjiang Petroleum Geology*, 25(6), 631-633.
- Heydari, E. (2003). Meteoric versus burial control on porosity evolution of the Smackover Formation. *American Association of Petroleum Geologists Bulletin*, 87(11), 1779-1797. DOI: [10.1306/07070302009](https://doi.org/10.1306/07070302009)
- Huang, S.J. (1990). Cathodoluminescence and diagenetic alteration of marine carbonate minerals (in Chinese with English abstract). *Sedimentary Geology and Tethyan Geology*, 4, 9-15.
- Huang, S.J. (1997). A study on carbon and strontium isotopes of Late Paleozoic carbonate rocks in the Upper Yangtze Platform (in Chinese with English abstract). *Acta Geologica Sinica*, 71(1), 45-53.
- Huang, S.J., Liu, S.G., Li, G.R., Zhang, M. and Wu, W.H. (2004). Strontium isotope composition of marine carbonate and the influence of diagenetic fluid on it in Ordovician (in Chinese with English abstract). *Journal of Chengdu University of Technology (Science & Technology Edition)*, 31(1), 1-7.
- Huang, S.J., Shi, H., Mao, X.D., Zhang, M., Shen, L.C. and Wu, W.H. (2002). Evolution of Sr Isotopes of the Cambrian Sections in Xiushan, Chongqing and Related Global Correlation (in Chinese with English abstract). *Geological Review*, 48(5), 509-516.
- Huang, W.H., Yang, M., Yu, B.S., Fan, T.L., Chu, G.Z., Wan, H., Zhu, J.Q., Wang, X. and Wu, S.Q. (2006). Strontium isotope composition and its characteristics analysis of Cambrian-Ordovician carbonate in Tazhong district, Tarim basin (in Chinese). *Earth Science-Journal of China University of Geosciences*, 31(6), 839-845.
- Huang, S.J., Zhang, M., Sun, Z.L., Hu, Z.W., Wu, S.J. and Pei, C.R. (2006). Age calibration of carbonatite samples from the Triassic Feixianguan Formation, Well Luojia 2, eastern Sichuan by strontium isotope stratigraphy (in Chinese with English abstract). *Journal of Chengdu University of Technology (Science & Technology Edition)*, 32(1), 111-116.
- Huang, S.J., Qing, H.R., Huang, P.P., Hu, Z.W., Wang, Q.D., Zou, M.L. and Liu, H.N. (2008). Evolution of strontium isotopic composition of seawater from Late Permian to Early Triassic based on study of marine carbonates, Zhongliang Mountain, Chongqing, China (in Chinese). *Science in China (Series D)*, 51(4), 528-539.
- Jia, Z.Y. and Cai, Z.X. (2004). Carbonate paleo-weathered crust reservoirs (body) (in Chinese with English abstract). *Geological Science and Technology Information*, 23(4), 94-104.
- Jiang, M.S., Zhu, J.Q., Chen, D.Z., Zhang, R.H. and Qiao, G.S. (2001). Carbon and strontium isotope variations and responses to sea-level fluctuations in the Ordovician of the Tarim basin (in Chinese with English abstract). *Science in China (Series D: Earth Sciences)*, 44(9), 816-823. DOI: [10.1007/BF02907094](https://doi.org/10.1007/BF02907094)
- Jin, Z.J. and Cai, L.G. (2006). Exploration prospects, problems and strategies of marine oil and gas in China (in Chinese with English abstract). *Oil and Gas Geology*, 27(6), 722-730.
- Kang, Y.Z. (2007). Review and revelation of oil/gas discoveries in the Paleozoic marine strata of China (in Chinese with English abstract). *Oil and Gas Geology*, 28(5), 570-575.
- Keith, M.L. and Weber, J.N. (1964). Carbon and oxygen isotopic composition of selected limestones and fossils. *Geochimica et Cosmochimica Acta*, 28(10-11), 1786-1816. DOI: [10.1016/0016-7037\(64\)90022-5](https://doi.org/10.1016/0016-7037(64)90022-5)
- Kerans, C. (1988). Karst-controlled reservoir heterogeneity in Ellenburger Group carbonates of West Texas. *American Association of Petroleum Geologists Bulletin*, 72(10), 1160-183.
- Land, L.S. (1980). The isotopic and trace element geochemistry of dolomite: The state of the art (in concepts and models of dolomitization). *Special Publication Society of Economic Paleontologists and Mineralogists*, 28, 87-110. DOI: [10.2110/pec.80.28](https://doi.org/10.2110/pec.80.28)

- Lavoie, D. and Chi, G.X. (2006). Hydrothermal dolomitization in the Lower Silurian La Vieille Formation in northern New Brunswick: geological context and significance for hydrocarbon exploration. *Bulletin of Canadian Petroleum Geology*, 54(4), 380-395. DOI: [10.2113/gscpgbull.54.4.380](https://doi.org/10.2113/gscpgbull.54.4.380)
- Li, H.H., Wu, G.H., Wang, H.J., Zhang, L.P. and Wang, C.L. (2009). Structural evolution, Reservoir-forming and Exploration Field of Peripheral Area of the Hetianhe Gas Field in Tarim Basin. *Geoscience*, 23(4), 587-594.
- Li, Z.X. and Guan, S.P. (2001). Sedimentary cycle and Strontium, Carbon, Oxygen isotopes of the Silurian at Luguhu region in Ning lang county of western margin of Yangtze platform. *Journal of Palaeogeography*, 3(4), 69-76.
- Liu, C.G., Li, G.R., Zhu, C.L., Liu, G.Y. and Lu, Y.F. (2008). Geochemistry characteristics of carbon, oxygen and strontium isotopes of calcites filled in karstic fissure-cave in Lower-Middle Ordovician of Tahe Oilfield, Tarim Basin (in Chinese). *Earth Science-Journal of China University of Geosciences*, 33, 3, 377-386.
- Liu, G.D. (2007). Suggestions on secondary pioneering of Chinese oil and gas resources (in Chinese with English abstract). *Special Oil and Gas Reservoirs*, 14(1), 1-4.
- Liu, J. and Ji, H.B. (2008). Sr Isotope Characteristics and its Indicative Significance for Biogeochemistry (in Chinese with English abstract). *Journal of Capital Normal University (Natural Science Edition)*, 29(4), 67-73.
- Liu, J.Q., Li, Z., Huang, J.C. and Yang, L. (2012). Distinct sedimentary environments and their influences on carbonate reservoir evolution of the Lianglitag formation in the Tarim basin, Northwest China. *Science China: Earth Sciences*, 55(10), 1641-1655. DOI: [10.1007/s11430-012-4457-5](https://doi.org/10.1007/s11430-012-4457-5)
- Liu, X.P., Wu, X.S. and Zhang, X.Z. (2004). Geochemistry characteristics of carbon and oxygen isotopes of Ordovician carbonatite palaeokarst reservoir in the western region of Lungu, Tarim Basin (in Chinese with English abstract). *Journal of Xi An Shi you University (Natural Science Edition)*, 19, 4, 69-72.
- Liu, Z.B., Gao, S.L., Yue, Y., Huang, X.R., Liu, S.L., Wu, S.Q., Zhang, Z.P. and Yang, S.B. (2014). Formation and distribution of the Ordovician reservoir in Maigaiti slope, Tarim Basin (in Chinese with English abstract). *Acta Petrologica Sinica*, 35(4), 654-663.
- Loucks, R.G. (1999). Paleocave Carbonate Reservoirs: Origins, Burial-Depth Modifications, Spatial Complexity, and Reservoir Implications. *American Association of Petroleum Geologists Bulletin*, 83(11), 1795-1834.
- McArthur, J.M., Howarth, R.J. and Bailey T.R. (2001). Strontium isotope stratigraphy: lowess version 3: best fit to the marine Sr-isotope curve for 0-509 Ma and accompanying look-up table for deriving numerical age. *Journal of Geology*, 109(3), 155-170.
- Montanez, I.P. (1994). Late Diagenetic Dolomitization of Lower Ordovician Upper Knox Carbonates: A Record of the Hydrodynamic Evolution of the Southern Appalachian Basin. *American Association of Petroleum Geologists Bulletin*, 78(8), 1210-1239.
- Roger, J.B., Gregg, C.O. and Guo, Q.G. (2004). Strontium isotopic signatures of oil-field waters: Applications for reservoir characterization. *American Association of Petroleum Geologists Bulletin*, 88, 12, 1677-1704.
- Rosen, M.R., Miser, D.E., Starcher, M.A. and Warren, J.K. (1989). Formation of dolomite in the Coorong region, South Australia. *Geochimica et Cosmochimica Acta*, 53(3), 661-669. DOI: [10.1016/0016-7037\(89\)90009-4](https://doi.org/10.1016/0016-7037(89)90009-4)
- Ross, C.A. and Ross, J.R.P. (1995). North American Ordovician depositional sequences and correlations. In: Cooper, J.D., Droser, M.L., Finney, S.C., eds. *Ordovician Odyssey: Short Papers for the 7th international Symposium on the Ordovician System*. Pacific section SEPM, 77, 309-313.
- Shi, Z.S., Chen, K.Y. and S. He, 2005: Strontium, sulfur and oxygen isotopic compositions and significance of paleoenvironment of paleogene of Dongpu Depression.- *Earth Science*, 30, 4, 430-436 (in Chinese with English abstract).
- Shi, Z.J., Xia, W.Q., Wang, Y., Tian, X.S. and Wang, C.C. (2014). Characteristics and identification of paleokarst in the Maokou Formation in the southeastern Sichuan basin (in Chinese). *Acta Petrologica Sinica*, 30(3), 622-630.
- Shields, G.A., Carden, G.A.F., Veizer, J., Meidla, T., Rong, J.Y., Li, R.Y. (2003). Sr, C and O isotope geochemistry of Ordovician brachiopods: a major isotopic event around the Middle-Late Ordovician transition. *Geochimica et Cosmochimica Acta*, 67(11), 2005-2025.
- Su, Z.T., Chen, H.D., Lin, L.B., Zhao, J.X. and Xu, Q. (2010). Character of palaeokarst and its reservoirs significance of Ordovician Tabamiaoarea, Ordos (in Chinese with English abstract). *Xinjiang Geology*, 28(2), 180-185.
- Tao, S., Tang, D.Z., Zhou, C.Y., Li, F., Li, J.J., Zhang, W.Z. and Men, C.Z. (2009). REE geochemical characteristics and implication on sedimentary environments of lower assemblage source rocks in Chuandongnan-Qianzhong and adjacent area (in Chinese with English abstract). *Petroleum Geology and Recovery Efficiency*, 16(3), 41-47
- Tian, L., Cui, H.F., Liu, B.M., Zhang, N. and Liu, J. (2013). Types and Distribution of Ordovician Reservoirs in Maigaiti Slope, Tarim Basin (in Chinese). *Xinjiang Petroleum Geology*, 34(4), 309-413..
- Tritlla, J., Cardellach, E. and Sharp, Z.D. (2001). Origin of vein hydrothermal carbonates in Triassic limestones of the Espadán Ranges (Iberian Chain, E Spain). *Chemical Geology*, 172(3-4), 291-305. DOI: [10.1016/S0009-2541\(00\)00257-6](https://doi.org/10.1016/S0009-2541(00)00257-6)
- Veizer, J., Ala, D., Azmy, K., Bruckschen, P., Buhl, D., Bruhn, F., Carden, G.A.F., Diener, A., Ebneth, S., Godderis, Y., Jasper, T., Korte, C., Pawellek, F., Podlaha, O.G. and Strauss, H. (1999). 87Sr/86Sr, 13C and 18O evolution of Phanerozoic seawater. *Chemical Geology*, 161(1-3), 59-88.
- Walter, M.R., Veevers, J.J., Calver, C.R., Gorjan, P. and Hill, A.C. (2000). Dating the 840-544Ma Neoproterozoic interval by isotopes of strontium, carbon, and sulfur in seawater, and some interpretative models. *Precambrian Research*, 100(1-3), 371-433. DOI: [10.1016/S0301-9268\(99\)00082-0](https://doi.org/10.1016/S0301-9268(99)00082-0)
- Wang, B.Q. and Al-Aasm, I.S. (2002). Karst-controlled diagenesis and reservoir development: Example from the Ordovician main-reservoir carbonate rocks on the eastern margin of the Ordos basin, China. *The American Association of Petroleum Geologists Bulletin*, 86(9), 1639-1658.
- Wang, Y., Shi, Z.J. and C.Y. Hong, 2009: Research review and developmental trends of technology in karst reservoir exploration in China.- *Carsologica Sinica*, 30, 3, 334-340 (in Chinese with English abstract).
- Wen, H.G., Chen, H.R., Wen, L.B., Zhou, G., Feng, Q.P. and Li, S. (2014). Diagenetic fluids of paleokarst reservoirs in Carboniferous from eastern Sichuan Basin: Some evidences from fluid inclusion, trace element and C-O-Sr isotope (in Chinese). *Acta Petrologica Sinica*, 30(3), 655-666.
- Wu, G.H., Li, H.H., Zhang, L.P., Wang, C.L. and Zhou, B. (2012). Reservoir forming conditions of the Ordovician weathering crust in the Maigaitislope, Tarim basin, NW China (in Chinese with English abstract). *Petroleum Exploration and Development*, 39(2), 144-153.
- Xia, M.J., Dai, J.X., Zou, C.N., Wang, Z.C. and Tao, S.Z. (2007). Caledonian karst palaeogeomorphology and the forming condition of gas pool, southern Ordos basin (in Chinese with English abstract). *Petroleum Exploration and Development*, 34(3), 291-298, 315.
- Yan, Z.B., Guo, F.S., Pan, J.Y., Guo, G. and Zhang, R.. (2005). Application of C, O and Sr isotope composition of carbonates in the research of paleoclimate and paleoceanic environment. *Contributions to Geology and Mineral Resources Research*, 20(1), 54-55.
- Yang, H.J., Li, Y., Shan, J.Z., Jing, B., Feng, X.J., Wang, D.J., 2007: Controlled effort of rock physical properties to migration and accumulation process of oil and gas: An example from Maigaiti slope, Tarim basin, China.- *Acta Petrologica Sinica*, 23, 4, 823-830 (in Chinese with English abstract).
- Yang, H.J., Han, J.F. and Sun, C.H. (2011). A development model and petroleum exploration of karst reservoirs of Ordovician Yingshan Formation in the northern slope of Tazhong palaeouplift (in Chinese with English abstract). *Acta Petrologica Sinica*, 32(2), 199-205. DOI: [10.7623/syxb201102002](https://doi.org/10.7623/syxb201102002)

- Zhang, B., Zheng, R.C., Wang, X.B., Luo, Y., Li, W., Wen, H.G. and Hu, Z.G. (2011). Paleokarst and reservoirs of the Huanglong Formation in eastern Sichuan Basin (in Chinese with English abstract). *Petroleum Exploration and Development*, 38(3), 257-267.
- Zhang, K., Wang, D.R. and Bryan, G.H. (2004). Reservoir characterization of the Ordovician oil and gas pools in the Tahe oilfield, Tarim basin, Northwest China (in Chinese). *Petroleum Exploration and Development*, 31(1), 123-126.
- Zhang, Q.Y., Liang, B., Cao, J.W., Dan, Y., Li, S.Y., Li, J.R., Hao, Y.Z., 2015: Research of geochemistry characteristics of carbon and oxygen isotopes of Ordovician paleokarst reservoir in the east of Lungu-7, North Tarim Basin.- *Geological Science and Technology Information*, 34, 2, 52-56 (in Chinese).
- Zhao, G.W. (2013). Middle-Late Ordovician sea level changes in the Bachu area, Tarim basin, Xinjiang: Carbon, Oxygen and Strontium isotope records (in Chinese). PhD thesis. Jilin University, Jilin, 1-103.
- Zhao, W.Z., Shen, A.J., Hu, S.Y., Pan, W.Q., Zheng, J.F. and Qiao, Z.F. (2012). Types and distributional features of Cambrian-Ordovician dolostone reservoirs in Tarim Basin, northwestern China (in Chinese with English abstract). *Acta Petrologica Sinica*, 28(3), 758-768.
- Zheng, R.C., Hu, Z.G., Zheng, C., Chen, S.C. and Dai, L.G. (2008). Geochemical characteristics of stable isotopes in paleokarst reservoirs in Huanglong Formation in northern Chongqing eastern Sichuan area (in Chinese with English abstract). *Earth Science Frontiers*, 15(6), 303-311.
- Zheng, X.H. (1995). Petroleum geological characteristics and exploration proposals to Bachu-Maigaiti area of the west Tarim Basin (in Chinese with English abstract). *Experimental Petroleum Geology*, 17(2), 114-120.
- Zhou, X.Y., Yang, H.J., Li, Y., Wang, Y.H., Zeng, C.M., 2006: Cases of discovery and exploration of marine fields in China(Part 7): Hotanhe gas field in Tarim Basin.- *Marine Origin Petroleum Geology*, 11, 3, 55-62 (in Chinese with English abstract).
- Zhou, X.Y., Pang, X.Q., Li, Q.M., Pan, H., Xiang, C.F., Jiang, Z.X., Li, S.M., Liu L.F. (2010). Advances and problems in hydrocarbon exploration in the Tazhong area, Tarim Basin (in Chinese with English abstract). *Petroleum Science*, 7(2), 164-178.